Scientific Bulletin of the
Politehnica University of Timisoara
Transactions on Mechanics Special issue

The 6th International Conference on
Hydraulic Machinery and Hydrodynamics
Timisoara, Romania, October 21 - 22, 2004

INTRODUCTION TO CAVITATION IN HYDRAULIC MACHINERY

François AVELLAN, Professor
Laboratory for Hydraulic Machines, School of Engineering
EPFL Swiss Federal Institute of Technology Lausanne
Avenue de Cour 33 Bis, CH-1007, Lausanne, Switzerland
Tel.: +41 21 693 2524, Fax: +41 21 693 3554, Email: francois.avellan@epfl.ch

ABSTRACT

Design, operation and refurbishment of hydraulic turbines, pumps or pump-turbine are strongly related to cavitation flow phenomena, which may occur in either the rotating runner-impeller or the stationary parts of the machine. The paper presents the cavitation phenomena featured by fluid machinery including type of cavity development related to the specific speed of machines in both pump and turbine mode, the influence of the operating conditions, such as load, head and submergence. Therefore, for each type of cavitation illustrated by flow visualization made at the EPFL testing facilities, the influence of cavitation development on machine efficiency, operation and integrity are discussed.

KEYWORDS

Cavitation, Hydraulic Machinery and Systems, Model Testing

NOMENCLATURE

A	[m^2]	Area of the Flow Cross Section
$C = \frac{Q}{A}$	[ms^{-1}]	Mean Flow Velocity
Cm	[ms^{-1}]	Meridian Velocity Component
Cu	[ms^{-1}]	Circumferential Velocity Comp.
$Cp = \frac{p - p_c}{\rho E}$	[-]	Static Pressure Factor
D	[m]	Runner Reference Diameter
$E = gH_1 - gH_2$	[Jkg^{-1}]	Specific Hydraulic Energy
$Fr = \sqrt{\frac{E}{gD}}$	[-]	Froude Number
$NPSE$	[Jkg^{-1}]	Net Positive Suction Energy
P	[W]	Mechanical Power of the Machine
$P_h = \rho QE$	[W]	Machine Hydraulic Power
Q	[m^{3}s^{-1}]	Discharge
$R = \frac{D}{2}$	[m]	Runner Reference Radius
$U = \omega R$	[ms^{-1}]	Circumferential Velocity
$\vec{W} = \vec{C} - \vec{U}$	[ms^{-1}]	Relative Flow Velocity
Z	[m]	Elevation
Z_a	[m]	Elevation of the Tail Water Level
Z_{ref}	[m]	Machine Reference Elevation
e_{rd}	[-]	Factor of Specific Energy Losses for the Machine Draft Tube
k	[-]	Geometric Factor
g	[ms^{-2}]	Acceleration Due to Gravity
$gH = \frac{p}{\rho} + gZ + \frac{C^2}{2}$	[Jkg^{-1}]	Mean Specific Energy
$h_s = Z_r - Z_a$	[m]	Machine Setting Level
n	[s^{-1}]	Speed of Revolution
p	[Pa]	Absolute Static Pressure
p_a	[Pa]	Atmospheric Pressure
p_v	[Pa]	Vapor Pressure
gH_r	[Jkg^{-1}]	Specific Energy Loss
$\chi_E = \frac{p - p_v}{\rho E}$	[-]	Local Cavitation Factor

$\kappa = \frac{\psi_c}{\varphi^2}$	[-]	Cavitation Number
$\psi = \frac{2E}{\omega^2 R^2}$	[-]	Specific Hydraulic Energy Coeff.
$\psi_c = \frac{2NPSE}{\omega^2 R^2}$	[-]	Net Positive Suction Specific Hydraulic Energy Coeff.
$\psi_r = \frac{2gH_r}{\omega^2 R^2}$	[-]	Energy Loss Coefficient
η	[-]	Efficiency
$\varphi = \frac{Q}{\pi\omega R^3}$	[-]	Flow Coefficient
φ_0	[-]	Whirl Free Flow Coefficient
ρ	[kgm^{-3}]	Water Density.
σ	[-]	Thoma Number
σ_i	[-]	Value of σ corresponding to the onset of cavities
σ_0	[-]	Lowest value of σ for which the efficiency remains unchanged as compared to cavitation free op.
σ_1	[-]	Lowest value of σ as compared to cavitation free operation for which an efficiency drop of 1% is noticed
ω	[rads^{-1}]	Runner Angular Velocity

Subscripts and Superscripts

1	High Pressure Side of the Machine
2	Low Pressure Side of the Machine
c	Low Pressure Side of the Runner

1. INTRODUCTION

Design, operation and refurbishment of hydraulic turbines, pumps or pump-turbine are strongly related to cavitation flow phenomena, which may occur in either the rotating runner-impeller or the stationary parts of the machine. The economic trend to increase the specific power of the machine combined with the modern operating conditions to operate the machine over an extended range of discharge and specific energy challenges the scientific community to develop advanced knowledge of cavitation physics for this type of machines. The paper presents the cavitation phenomena featured by fluid machinery including type of cavity development related to the specific speed of machines in both pump and turbine mode, the influence of the operating conditions, such as load, head and submergence. Therefore, for each type of cavitation illustrated by flow visualization made at the EPFL testing facilities, the influence of cavitation development on machine efficiency, operation stability and integrity are discussed.

After introducing the general definitions and notations in use in the field of hydraulic machinery, we describe how the level setting of a hydraulic machine through so called cavitation tests of reduced scale models. Then we present for each type of machines, storage pumps or pump turbines, Francis turbines and Kaplan or Bulb turbine the different types of cavitation developments and the resulting performance alteration and risk of erosions.

2. MODEL TESTING

2.1. General definition and notation

We examine in this paper the case of reaction hydraulic machines including hydro-turbine, storage pump or pump-turbine. Irrespective of the flow direction, the subscript 1 defines the high pressure reference section of the machine and the subscript 2 the low pressure reference section, as defined Fig. 1. The low-pressure section of the runner is quoted with the subscript c.

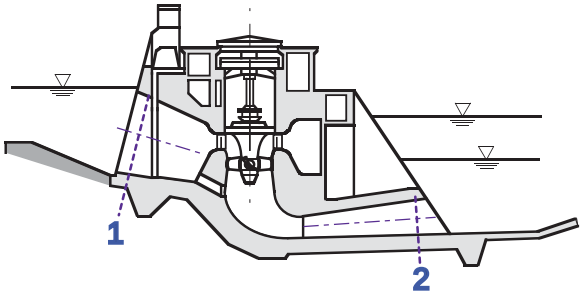

Fig. 1 General sketch of a run-off power plant with Kaplan Turbines.

By introducing p, the absolute pressure, Z, the elevation of a point and C the mean velocity defined by the ratio between the discharge Q and the section area A, gH, the mean specific hydraulic energy of a given flow passage cross section, is defined as:

$$gH = \frac{p}{\rho} + gZ + \frac{C^2}{2} \quad [\text{Jkg}^{-1}]$$

where ρ is the water density and g the gravity acceleration.

Therefore, the specific hydraulic energy E of the machine is defined as the difference of the mean specific energy values between the high and the low-pressure limiting sections of the machine.

$$E = gH_1 - gH_2$$

The breakdown of the expression of the mean specific hydraulic energy gives the following expression for E :

$$E = \left[\frac{p_1}{\rho} + gZ_1 + \frac{C_1^2}{2}\right] - \left[\frac{p_2}{\rho} + gZ_2 + \frac{C_2^2}{2}\right] \quad [\text{Jkg}^{-1}]$$

The product of the discharge by the machine specific energy then defines the hydraulic power P_h of the machine

$$P_h = \rho Q E \qquad [\text{W}]$$

The mechanical power P of the machine including the mechanical power dissipated in guide bearings, thrust bearings and shaft seals of the hydraulic machine, is related to the hydraulic power by the overall efficiency, η, of the machine by the following definitions:

$\eta = \frac{P_h}{P}$ for a pump and $\eta = \frac{P}{P_h}$ for a turbine.

Geometrical and kinematical similarity principles allow defining the dimensionless terms, which determine the hydraulic characteristics of the machine.

The angular velocity ω and the reference radius R of the machine runner/impeller define the reference area πR^2 and the reference specific kinetic energy $\frac{1}{2}\omega^2 R^2$, which in turns provide the definition of φ and ψ, the dimensionless discharge and energy coefficients.

$$\varphi = \frac{Q}{\pi \omega R^3} \qquad\qquad \psi = \frac{2E}{\omega^2 R^2}$$

All along this paper, we will use preferably these coefficients since they are conveniently directly proportional to the discharge Q and the specific energy E .

Therefore, for any machine at a given α setting, the opening angle of the guide vanes the discharge-energy relations will collapse to a single function whatever the runner/impeller rotational speed. For every opening angle α, we can plot the φ - ψ characteristic as per Fig. 2;

$$\psi = \psi(\varphi, \alpha)$$

Thus, the set of discharge and specific energy coefficients, φ, ψ, and, α, the opening angle of the guide vanes, defines the operating conditions, for which we can express the efficiency :

$$\eta = \eta\ (\varphi, \psi, \alpha)$$

In a similar way, we can plot on the diagram, φ - ψ, the contours of efficiency iso-values to define the so-called efficiency hill chart of the machine, see Fig. 2.

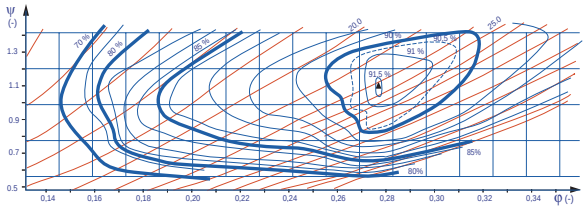

Fig. 2 Typical hill chart of a Francis turbine, $\nu = 0.500$.

For real flow, viscous and turbulence dissipation influences the machine efficiency and leads to the so-called scale effect between reduced scale model and full-scale prototype.

2.2. General Model tests

According to IEC 60193 standard, [1], model tests require that the geometric, the kinematics and the dynamic similitude principles be fulfilled between model and prototype. Model dimensions must be sufficient to achieve an excellent geometrical similarity with the prototype; the typical outlet diameter D of Francis and Kaplan runners is of the order of 0.3 - 0.4 m. Test installations should fulfill requirements of the IEC standards regarding their capacity.

As an example, a view of the PF1 EPFL universal test rig for all types of reaction machines, turbines, pumps and pump-turbines is reported Fig. 3. This test rig has a 900 kW maximum pumping power, leading to test heads of up to 100 m (1'000 Jkg^{-1}) and a maximum flow rate of 1.4 m^3/s. The dynamometer is limited to a 320 kW maximum generated power at 2'500 rpm.

In general, a test procedure consists in measuring:

- the overall hydraulic characteristic of the machine and the corresponding efficiency hill chart over a wide range of operating conditions;
- guaranteed operating point efficiencies and power output;
- cavitation characteristics;
- pressure fluctuations at the draft tube inlet, at the spiral case inlet and on the head cover of the machine;
- runaway speed ;
- index test and flow velocity distribution in various locations.

In addition, mechanical measurements are often carried out, such as torque and bending moment on guide vanes, runner axial thrust etc....

A hill chart corresponding to the model test of a typical Francis hydro-turbine is reported Fig. 2.

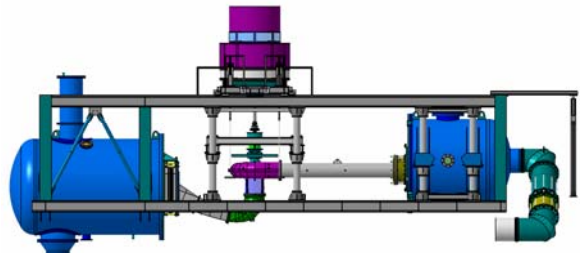

Fig. 3 Reduced Scale Model of a Francis Turbine installed on the EPFL PF1 Test Rig

2.3. Standard cavitation tests

Standard cavitation tests consist in investigating the influence of cavitation development on the hydraulic characteristics and the type of cavity susceptible to develop during the operation of the prototype machine.

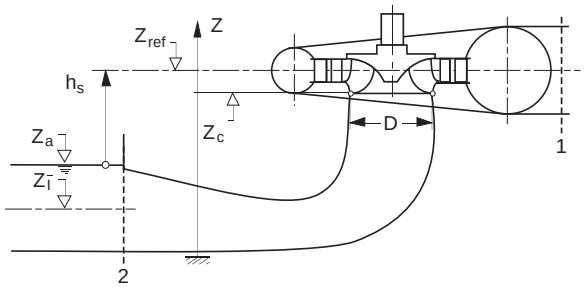

Fig. 4 Setting level definitions for a hydraulic machine

These investigations are very important for the evaluation of the setting level h_s of the machine to the tail-water level Z_a, see Fig. 4, defined as:

$$h_s = Z_r - Z_a \quad \text{(m)}$$

According to the IEC standard nomenclature, the Net Positive Suction specific Energy, $NPSE$, of a hydraulic machine is the difference of the specific energy at Section 2, with the specific energy due to the vapor pressure p_v, referred to the reference level Z_{ref} of the machine.

$$NPSE = gH_2 - \frac{p_v}{\rho} - gZ_{ref} = \left[\frac{p_2}{\rho} + gZ_2 + \frac{C_2^2}{2}\right] - \frac{p_v}{\rho} - gZ_{ref} \quad (\text{Jkg}^{-1})$$

For a turbine, it can be assumed that all the specific kinetic energy at the turbine outlet is dissipated in the tail race water channel therefore $NPSE$ can be approximated as follows,

$$NPSE \approx \frac{p_a}{\rho} - \frac{p_v}{\rho} - gh_s + \frac{C_2^2}{2} \quad (\text{Jkg}^{-1})$$

Meanwhile for a storage pump or a pump-turbine in pumping mode, the intake of the machines should have negligible specific energy losses and therefore the $NPSE$ can be approximated as follows

$$NPSE \approx \frac{p_a}{\rho} - \frac{p_v}{\rho} - gh_s \quad (\text{Jkg}^{-1})$$

Depending on the reference quantities chosen either the Thoma's cavitation factor σ, so called Thoma number or the net positive suction specific energy coefficient ψ_c can be chosen to define a dimensionless cavitation number.

$$\sigma = \frac{NPSE}{E}, \quad \psi_c = \frac{2NPSE}{\omega^2 R^2}$$

In both cases, we can observe that these terms are simply related to the setting level h_s, which is easily determined. However, the problem arises in estimating the static pressure at the low-pressure section c of the runner. The mean specific energy conservation law between these sections leads to the following expression for the absolute pressure p_c,

$$\frac{p_c - p_v}{\rho} = NPSE + g\left(Z_{ref} - Z_c\right) - \frac{C_c^2}{2} + E_{rd} \quad (\text{Jkg}^{-1})$$

where E_{rd} is the mean specific energy losses between the sections c and 2 of the draft tube. According to the flow direction, these losses are positive for a turbine and negative for a pump.

The corresponding dimensionless expression allows introducing a local cavitation factor χ_E related to σ as follows

$$\chi_E = \frac{p_c - p_v}{\rho E} = \sigma + \frac{1}{Fr^2}\left(\frac{Z_{ref} - Z_c}{D}\right) - \frac{C_c^2}{2E} + e_{rd}$$

where the Froude number is defined as

$$Fr = \sqrt{\frac{E}{gD}}$$

The necessary condition of cavity onset $p = p_v$ in the runner is then, expressed by the condition:

$$Cp = -\chi_E$$

with the pressure factor defined as:

$$C_p = \frac{p - p_c}{\rho E}$$

Thus, it is apparent that the static pressure will strongly depend on the operating point of the machine, even though the Thoma cavitation number is kept constant. This can be shown by introducing the discharge coefficient φ of the machine.

For a turbine we have:

$$\chi_E = \sigma + \frac{1}{Fr^2}\frac{Z_{ref} - Z_c}{D} - \frac{\varphi^2 + \left(1 - \frac{\varphi}{\varphi_0}\right)^2}{\psi} + e_{rd}$$

where φ_0 corresponds to the discharge operation with minimum whirl.

Therefore, from the expression of the cavitation factor χ_E we see that as much the discharge is increased, the pressure decreases up to reach the pressure vapor. For this extreme condition we have:

$$\chi_E = 0$$

For the case of reference taken at the runner outlet, by neglecting the draft tube loss factor and assuming a whirl free condition we have:

$$\chi_E = 0 \approx \sigma - \frac{\varphi^2}{\psi} \text{ leading to } \frac{\psi_c}{\varphi^2} \approx 1 .$$

Therefore, the above ratio allows us to introduce κ the dimensionless cavitation number, which expresses the margin to vapor pressure that we have for a turbine.

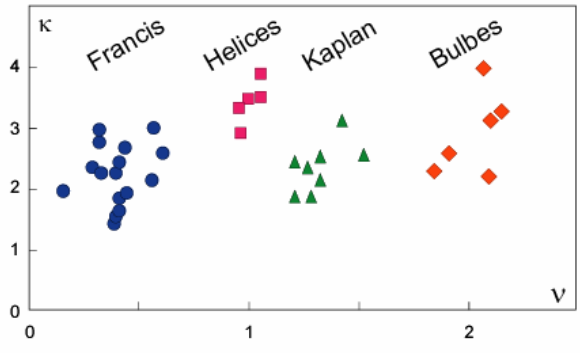

Fig. 5 κ cavitation number as a function of specific speed for the turbines taken from [18]

We have reported Fig. 5 the κ values corresponding to the specific speed of turbines taken from [18]. We see that in practice, the setting of a turbine requires that κ r fulfill the condition:

$$\kappa = \frac{\varphi^2}{\psi} \geq 1.8$$

For a pump with a pure axial inlet flow, we have in the same way

$$\chi_E = \sigma + \frac{1}{Fr^2}\frac{Z_{ref} - Z_c}{D} - \frac{1}{k}\frac{\varphi^2}{\psi} + e_{rd} ,$$

where k is a pure geometric factor to take into account that the reference section can be arbitrarily selected. In the case of a reference section taken at the impeller eye, this factor reduces to unity.

$$k = k_c = 1$$

So, in both types of machines the local value of the cavitation coefficient is strongly affected by the discharge coefficient φ. We can observe that for a given operating point, cavitation tests are in similitude with the prototype flow provided the Thoma numbers and the Froude numbers are the same in both cases, model scale and prototype scale. Owing to the scale length factor between the prototype and the model of large units, it is often impossible to fulfill the Froude similarity requirement. For example, if we consider a runner diameter of 5 m operating at 500 Jkg^{-1} and the runner diameter of the corresponding model being 0.4 m, the Froude similitude leads to a test specific energy of 40 Jkg^{-1}, which is far too low for testing. Thus, very often the test head is higher than the corresponding Froude head and in turns the cavity vertical extension on the blades is squeezed by the scale effects. A way to overcome as much as possible the influence of the Froude number is to define a reference level of the machine as close as possible to the elevation where cavity development takes place. Therefore, for vertical axis machines it is strongly recommended to define the low pressure elevation level Z_c as a reference.

Nevertheless, standard cavitation tests are performed for different operating points by keeping constant the specific energy coefficient ψ and following the influence of the Thoma number σ on the efficiency η and the discharge coefficient φ. Typical $\eta - \sigma$ curves for a Francis turbine are reported Fig. 6.

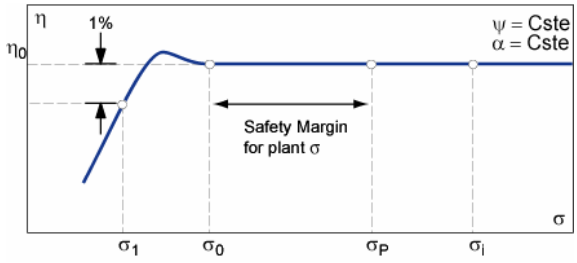

Fig. 6 Cavitation curve for a Francis turbine, by keeping constant the machine specific energy coefficient and for a given guide vane opening angle.

While σ is decreased, observations of the cavitation onset and the cavity development are reported. Characteristic values of σ are defined such as:

- σ_i : onset of visible cavities;
- σ_0 : lowest value of sigma for which the efficiency remains unchanged;
- σ_1 : 1% drop of efficiency.

2.4. Type of Cavitation and Setting Level

The objective of cavitation tests being to determine the setting level of the machine in order to overcome any efficiency alteration and to minimize the erosion risk, each type of cavitation is considered with respect to its dependence on the value of the setting level and to the erosion risk.

On the one hand, the onset of a leading edge cavity is more influenced by the blade geometry and the flow incidence angle than the value of σ. This means that increasing to a very high value of σ in order to prevent a leading edge cavity development will cause unacceptable costs. Thus, this type of cavity, which cannot be avoided for off-design operation, has to be considered with respect to the erosion risk. In this case, the Thoma number is determined according to an acceptable cavity development.

On the other hand, cavity development corresponding to the design operating point such as bubble cavitation and hub cavity are very sensitive to the Thoma number value. However, for each case of hydraulic machine, different types of cavitation arise depending either on the blade design and the operating point or on the Thoma number value. Thus, it is important to examine, for each case of hydraulic machine, the type of cavitation, which occurs in the operating range.

3. CENTRIFUGAL PUMPS

3.1. Type of Cavitation

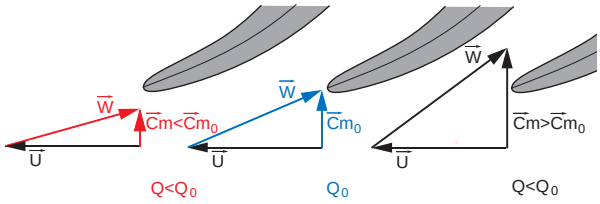

Fig. 7 Influence of the discharge value on the flow velocity triangle at the impeller inlet

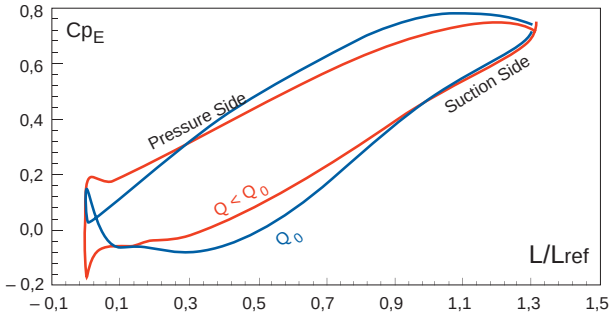

Fig. 8 Computation of pressure distribution along the mid span streamline of a storage pump impeller for Q_0 and $Q < Q_0$, taken from [9].

Cavity development in a centrifugal pump is fully controlled by the discharge coefficient according to the relative flow velocity incidence angle at the impeller inlet, Fig. 7, which strongly affects the pressure distribution on the blades at the inlet, [9], Fig. 8.

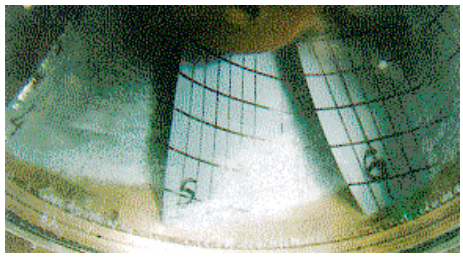

Fig. 9 Traveling bubble development in a storage pump impeller, $Q = Q_0$, during model testing.

At the rated discharge, traveling bubble cavitation can be observed on the suction side of the blades, Fig. 9. This type of cavity corresponds to a low incidence angle of the flow and depending on the design of the impeller, the minimum of pressure being at the impeller throat.

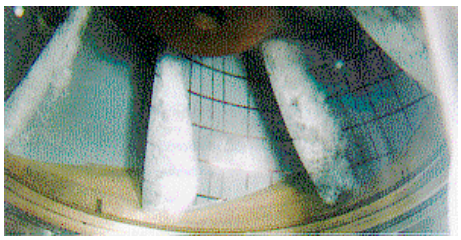

Fig. 10 Leading edge cavity development in a storage pump impeller, $Q < Q_0$, during model testing.

For a lower discharge value, the flow incidence is increased and then, a leading edge cavity appears, as shown Fig. 10.

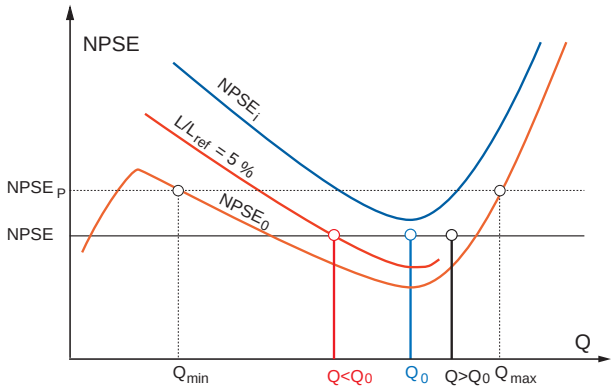

Fig. 11 Influence of the discharge value on a storage pump NPSE.

For low values of σ, cavitation vortices can be observed at the inlet of the runner coming from the leakage flow through the shroud seal, Fig. 9.

3.2. Efficiency Alteration

Alteration of efficiency is due to the cavity extension up to the throat of the flow passage in the impeller. However, before this efficiency alteration, cavitation erosion can occur at the closure region of the cavity and can be dramatically increased when transient cavities are advected downstream of the impeller throat. For high discharge coefficient value, leading edge cavities are developing at the pressure side of the impeller blades leading to a rapid drop of the efficiency.

The influence of the cavitation development on the pump efficiency can be seen from the cavitation curves drawn for different discharge values, Fig. 12.

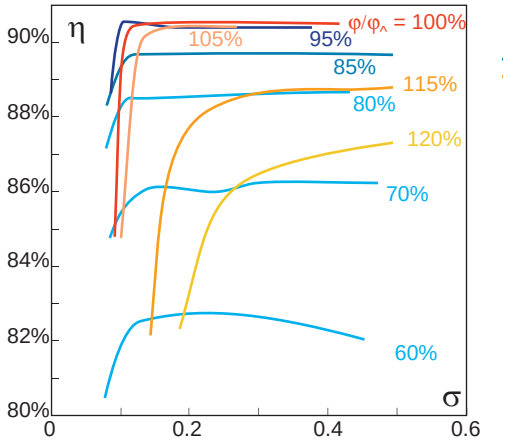

Fig. 12 Cavitation curves for a centrifugal pump for different discharge coefficient values

3.3. Cavitation Erosion

In a centrifugal pump, leading edge cavity is the main type of cavitation development over a wide operating range of discharge. Then the setting level of the machine is selected by evaluating the erosion risk in the full operating range since for any reasonable value of σ, a leading edge cavity still exists for a sufficiently low value of the discharge value.

In general cavitation erosion are observed on pump impellers on the blade suction sides, 0 shaded area A. Depending on how well the incoming flow is controlled, erosion can be observed either on the hub wall, 0 shaded area C, or on the wall of the impeller shroud, if any, 0 shaded area B.

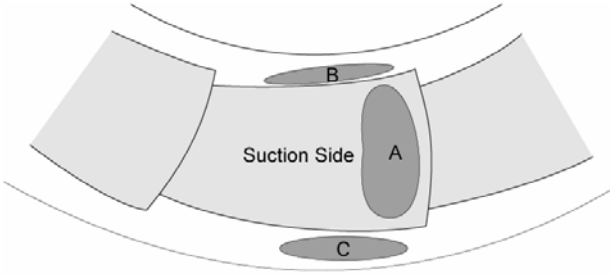

Fig. 13 Typical eroded areas of a pump impeller.

A very good correlation is obtained between the cavity development observations made during model tests and the field observations of the eroded area on the corresponding prototype impeller, Fig. 14.

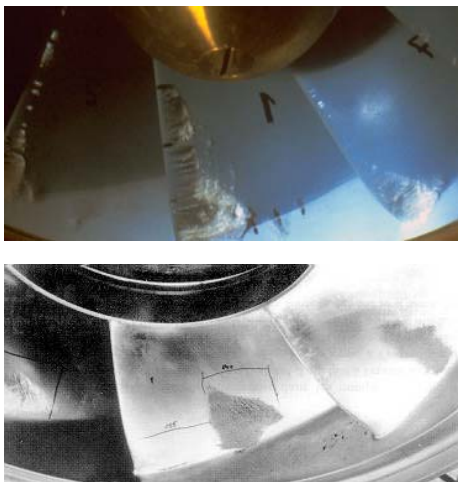

Fig. 14 Cavitation erosion of a storage pump impeller compared to the leading edge cavitation development as observed during testing of the homologous reduced scale model.

In the case of unshrouded impellers, tip clearance cavities appear and can erode either the pump casing or the blades themselves.

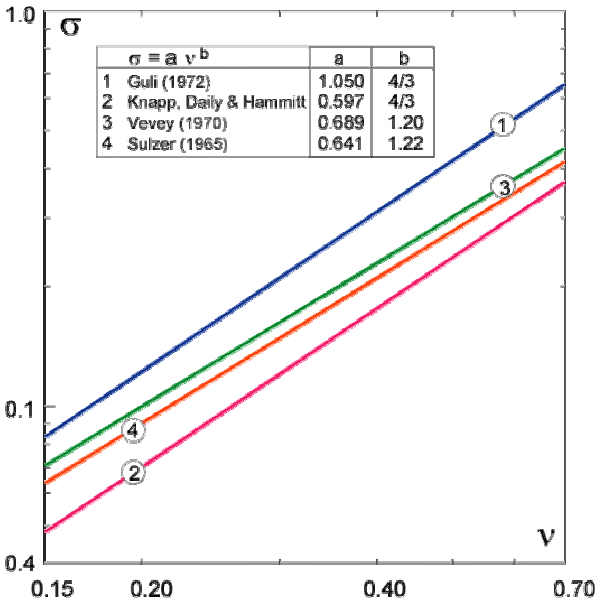

Fig. 15 Statistical acceptable values of Thoma cavitation number as a function of pump specific speeds.

Statistical values of power statistical relation between the acceptable value of the Thoma cavitation number and the pump specific speed are provided Fig. 15.

4. FRANCIS TURBINES

4.1. Type of Cavitation

In the case of a Francis turbine and for the design operating range, the type of cavity developing in the runner is closely driven by the specific energy coefficient ψ, the flow coefficient φ influencing only the cavity whirl.

Fig. 16 Inlet edge cavitation, Francis turbine.

High and low values of ψ correspond to a cavity onset at the leading edge suction side and pressure side of the blades respectively, see Fig. 16. This type of cavitation is not very sensitive to the value of the Thoma number and it can lead to a severe erosion of the blades.

Fig. 17 Traveling bubble cavitation in a Francis turbine runner.

Traveling bubble cavitation takes place for the design value of ψ, at the throat of the runner flow passage, close to the outlet and corresponds to low flow angles of attack. This type of cavitation, see Fig. 17, is very sensitive to the content of cavitation nuclei and to the value of the Thoma number. For this reason, the plant NPSE is determined with respect to this type of cavitation. The drop of the η-σ curve is noticed when cavities extend up to the runner outlet in both types of cavitation.

Depending on the value of the flow coefficient φ, a whirl cavity develops from the hub of the runner to the center axis of the draft tube in the bulk flow, as shown Fig. 18. The size of the cavity is dependent of σ, but the vortex motion depends only on the

flow coefficient values. According to the outlet flow velocity triangle of Fig. 18, inverse runner rotation of the vortex corresponds to high flow regime and leads to a large axi-symmetric fluctuating cavity. In turn, low flow regimes are responsible for a helical shape of the whirl, rotating at a speed, between 0.25 and 0.4 times the runner rotational frequency. The whirl development is mainly concerned with the stability of machine operation, since it is the main source of pressure fluctuations in the hydraulic installation [20][21].

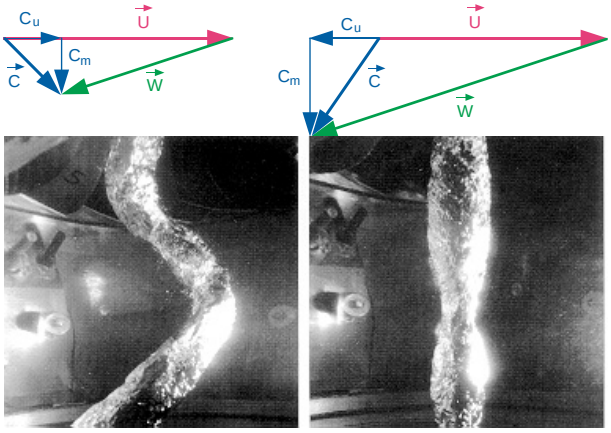

Fig. 18 Cavitation whirl at low and high discharge operation, in a Francis turbine discharge ring.

At low flow regime, one can observe complex flow recirculation at the inlet of the runner leading to vortex cavitation attached to the hub and extending up to the blade to blade passage, see Fig. 19. This type of turbine operation corresponds usually to off-design operation. However this operation cannot be avoided during for instance the reservoir filling up period of a new hydro-power generation scheme.

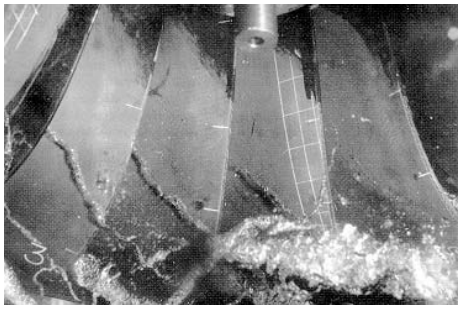

Fig. 19 Inter blades cavitation vortices in a Francis turbine runner.

The different limits corresponding to the development of each type of cavitation are reported in the hill chart of Fig. 20.

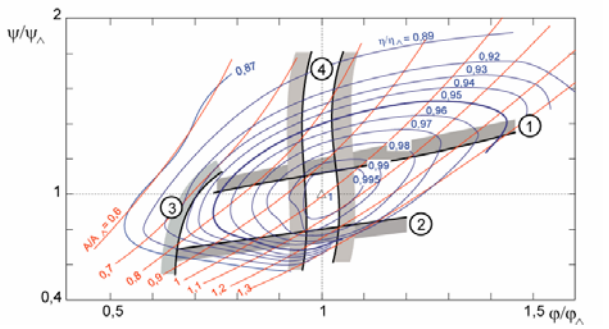

Fig. 20 Limits of cavitation development within the operating range of a Francis turbine:
1-Suction side leading edge cavitation limit;
2-Pressure side leading edge cavitation limit;
3-Interblade cavitation vortices limit;
4-Discharge ring swirl cavitation limits.

4.2. Efficiency Alteration

The setting of a Francis turbine is determined according to the risk of efficiency alteration, which is higher for high discharge, or high load, operating conditions as it can be seen from the expression of the cavitation factor χ_E. Therefore, the runner is usually designed in such a way that this corresponds to the development of traveling bubble outlet cavitation, Fig. 17. This type of cavitation is very sensitive to the content of cavitation nuclei and to the value of the Thoma number, [17]. For this reason, the plant NPSE is determined with respect to this type of cavitation.

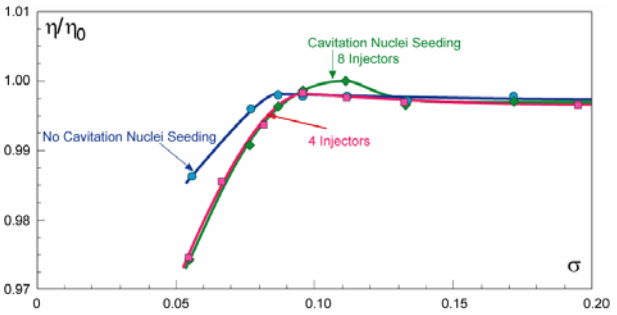

Fig. 21 Influence of free stream nuclei content on efficiency cavitation curves.

However, many tests carried out at EPFL, [4][16], for Francis turbine of different specific speeds confirm a strong influence of cavitation nuclei content combined with the test head on the efficiency alteration phenomenon by cavitation, Fig. 21 and Fig. 23. Nuclei content does not only influence cavitation inception, [19], but also the development of bubble traveling cavities [3].

Moreover, test head influence is found to be more related to an effect of the active nuclei content than of the Froude effect. According to the Rayleigh

Plesset stability analysis the lower radius limit of an active nucleus depends directly on the test head value leading to more or less active nuclei for a given nuclei distribution.

The cavitation curves reported Fig. 21, are obtained according to the usual cavitation tests. In addition, air micro-bubbles are seeded in the upstream vessel in order to vary the free stream cavitation nuclei content. It can be observed that, for a given threshold value of the nuclei content, the efficiency is no longer affected by increasing the nuclei content, the cavitation coefficient being kept constant.

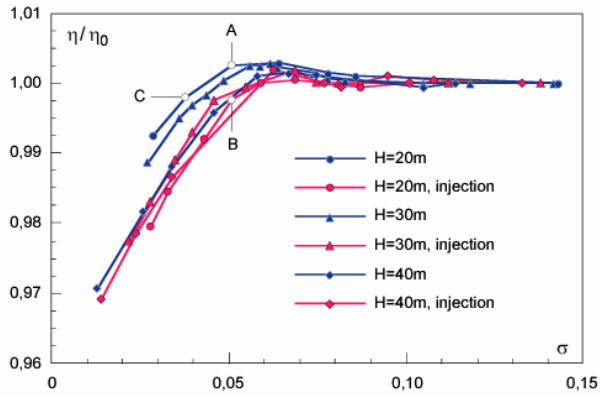

Fig. 22 Influence of head and cavitation nuclei content on Francis turbine cavitation curves

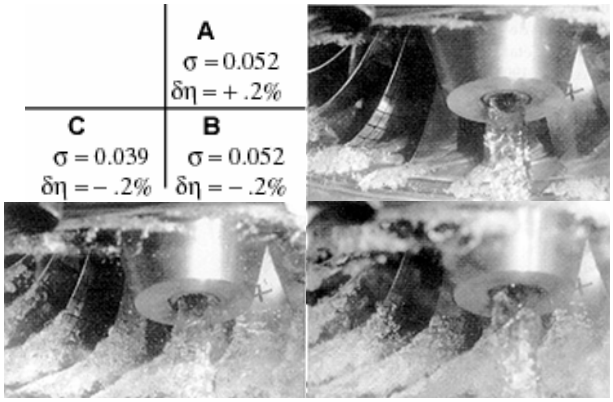

Fig. 23 Flow visualization of traveling bubble cavitation developments corresponding to the A, B & C points of Fig. 23.

Moreover, the efficiency alteration is strongly related to the cavitation extent on the blade as it is confirmed by flow visualizations. Photographs reported Fig. 23, correspond to the cavitation curves of a test head of 20 m in order to overcome any Froude effect on the cavity extent. Photographs A, B are taken for the same low σ value of 0.052 and correspond to a low nuclei content and to a saturated state, respectively. One can observe that the performance alteration is mainly due to the vaporization of a part of the blade to blade channel region which is under the vapor pressure. Thus, the saturation phenomenon occurs when the active nuclei amount is large enough to occupy all this region.

Evidence of the strong dependency between the volume of vapor and efficiency drop can be found in comparing the photographs B and C, taken for closely the same efficiency drop of 0.2 %. Even though, the sigma value of point C, σ = 0.039, is rather lower than the σ value of case B, the nuclei content in the case C is small enough to lead to a same volume of vapor and then to the same performance drop.

The drop of the η-σ curve is noticed when cavities extend up to the runner outlet in both types of cavitation.

Statistical values of power statistical relation between the acceptable value of the Thoma cavitation number and the specific speed are provided Fig. 24 for a Francis turbine.

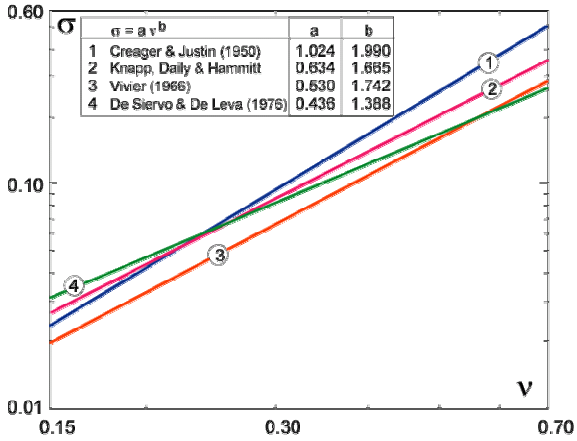

Fig. 24 Statistical acceptable values of Thoma cavitation number as a function of Francis turbine specific speeds.

4.3. Cavitation Erosion

Typical runner areas where cavitation erosion can be observed are reported Fig. 25.

In general severe cavitation erosion damages are observed in Francis runners on the blade suction sides, shaded area A of Fig. 25 or downstream in the blade to blade channel, shaded area B of Fig. 25.

The cause of those types of erosion, Fig. 26 and Fig. 27, is due to unexpected leading edge cavitation development Fig. 16 and can only be corrected by reshaping the inlet edge. However, wall erosion can be mitigated by welding a layer of cavitation resistant alloy.

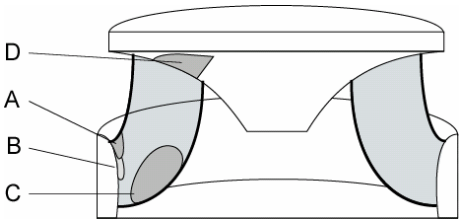

Fig. 25 Typical eroded areas of a Francis runner.

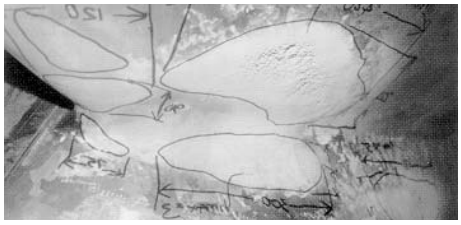

Fig. 26 Typical erosion at the wall of the blade suction side due to inlet edge cavitation, shaded area A of Fig. 25.

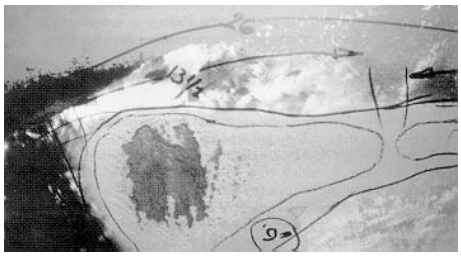

Fig. 27 Typical erosion at the wall of the blade suction side due to inlet edge cavitation, shaded area B of Fig. 25.

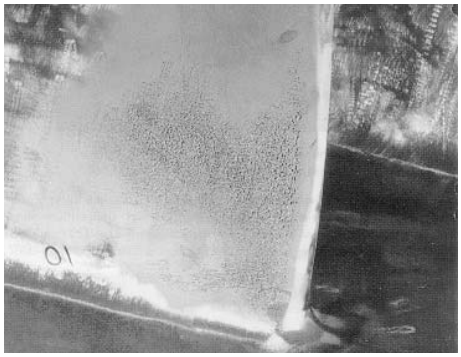

Fig. 28 "Frosted" area at the wall of the runner blade trailing edge due to outlet traveling bubble cavitation, shaded area C of Fig. 25.

In case of development of traveling cavitation bubble at the runner outlet region, Fig. 17, a "frosted" area can be observed, shaded area C of Fig. 25., which usually leads to barely visible erosion, Fig. 28, and is easily controlled by the Thoma cavitation number.

Finally, low load inter-blade cavitation vortices, Fig. 19, can lead to erosion of the runner hub wall, shaded area D of Fig. 25 and Fig. 29.

Fig. 29 Typical erosion at the wall of the runner hub due to inter-blades cavitation vortices, shaded area D of Fig. 25.

5. KAPLAN AND BULB TURBINES

5.1. Type of Cavitation

Runners of Kaplan and bulb turbines are axial with adjustable blade pitch angle and the control of both the guide vane opening and the blade pitch angle allows optimized operation of the machine, so called "on cam" operation.

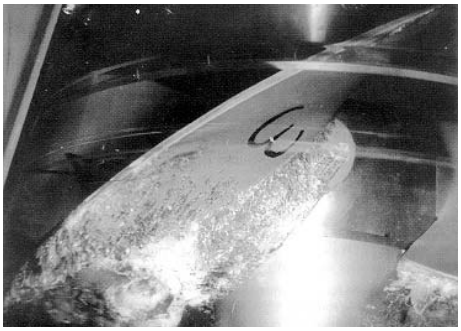

Fig. 30 Hub cavitation development for a Kaplan runner

Fig. 31 Tip clearance and hub cavitation for a Kaplan runner

For the design operating range a cavity development takes place at the hub of the runner, Fig. 30. This type of cavitation is very sensitive to the Thoma number. Any effect of the water cavitation nuclei content is observed for this type of cavitation [14]. However, the air entertainment can

have a great influence on the extent of this cavity, [22].

Since the blades are adjustable, the runner is not shrouded and, then as shown Fig. 31, tip clearance cavitation takes place in the gap between the blades and the machine casing, leading to an erosion risk even though the head could be low. This type of cavitation is driven by the flow shear layer in this gap and it is not very dependent of the Thoma cavitation number.

Even for the case of on cam operation, leading edge cavities can be observed at the inlet of the runner but can be avoided by improving the shape of the blade leading edge [12].

The different zones in the hill chart corresponding to each type of cavitation development are reported Fig. 32.

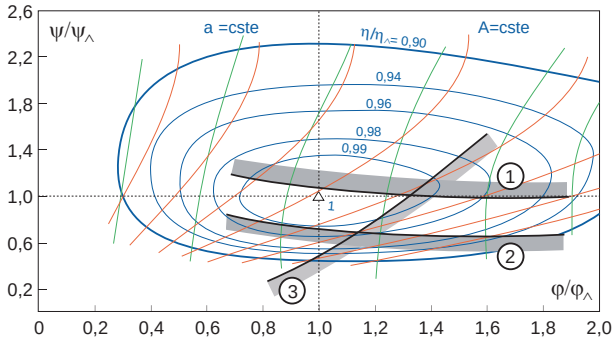

Fig. 32 Limits of cavitation development within the operating range of a Kaplan turbine;
1-Leading edge suction side cavitation limit,
2-Leading edge pressure side cavitation limit,
3-Hub cavitation limit.

5.2. Efficiency Alteration

The efficiency alteration for a Kaplan and bulbs turbines is mainly due to the development of hub cavitation, Fig. 30.

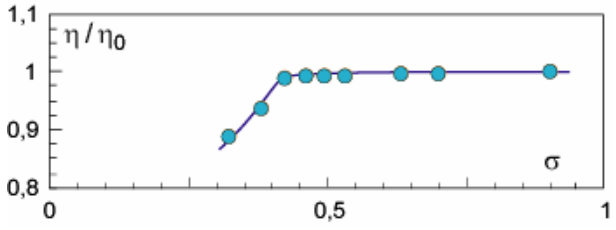

Fig. 33 Efficiency cavitation curve for a Kaplan Turbine.

As this hub cavity reaches the blade trailing edge, we can notice an efficiency drop, Fig. 33. This type of cavitation has already mentioned is very sensitive to the Thoma number and determines the plant NPSE of the machine.

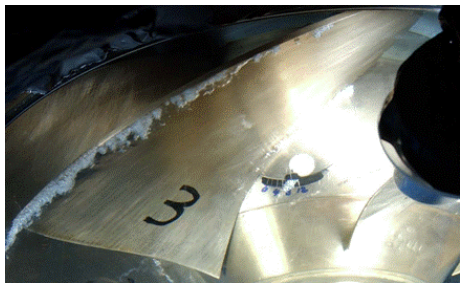

Fig. 34 Cavitation development for σ_{Plant}

Depending on the head of the machine limited development of tip clearance cavitation can be admissible for plant NPSE, Fig. 34

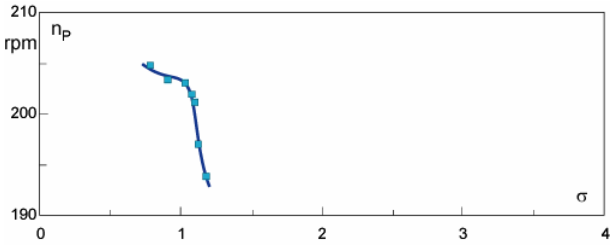

Fig. 35 Influence of Thoma cavitation number on Kaplan runaway speed.

Especially for the case of Kaplan or bulb turbines, it can be noticed a strong influence of the Thoma cavitation number on the runaway speed, Fig. 36.

Statistical values of power statistical relation between the acceptable value of the Thoma cavitation number and the specific speed are provided Fig. 36 for Kaplan turbines.

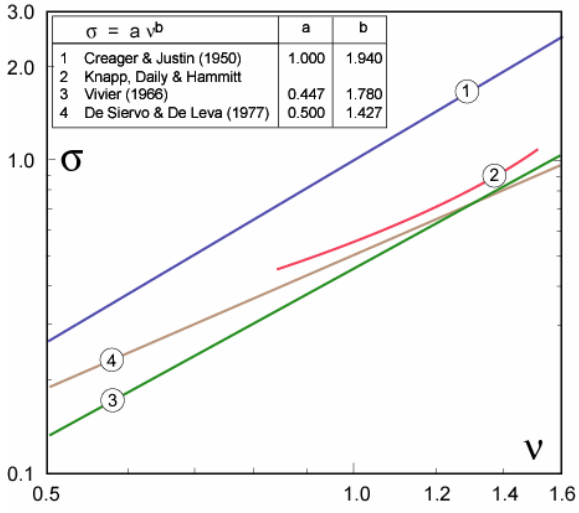

Fig. 36 Statistical acceptable values of Thoma cavitation number as a function of Kaplan turbine specific speeds.

5.3. Cavitation Erosion

Typical Kaplan runner areas where cavitation erosion can be observed are reported Fig. 37

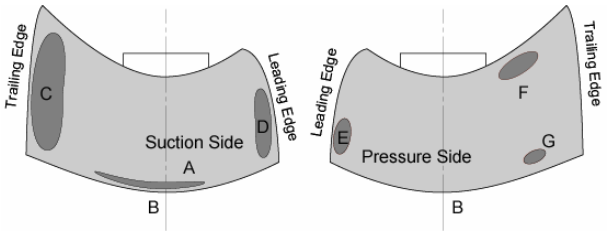

Fig. 37 Typical eroded areas of a Kaplan runner.

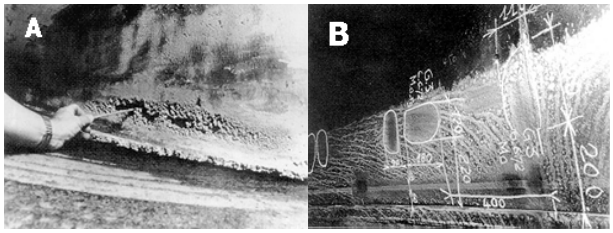

Fig. 38 Typical erosion at the tip of the runner blade and at the discharge ring due to inter-blades cavitation vortices, shaded area D of Fig. 25.

The most critical area where cavitation erosion is observed are the blade tips and the machine casing, shaded area A and B of Fig. 37. This erosion, Fig. 38, is due to the development of tip clearance cavitation, which can take place even at plant NPSE, Fig. 34.

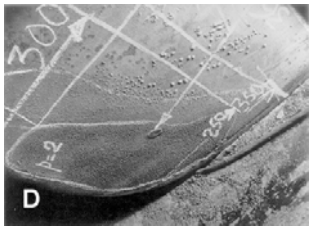

Fig. 39 , Typical erosion at the suction side of the blade due to leading edge cavitation, shaded area E of Fig. 25.

Either for lasting operations at high head or at low head erosion takes place at the suction side or the pressure side of the runner inlet, dashed area D or E of Fig. 37 respectively. This type of erosion is caused by inlet edge cavitation, Fig. 39. Erosion corresponding to dashed area F or G of Fig. 37 can occurs during lasting low head operation. Finally,h for high load operation conditions erosion can be observed at the outlet of the runner at the suction side, shaded area C of Fig. 37

CONCLUSION

A survey of the different types of caviation featured by hydraulic machinery has been carried out. This survey finally emphasizes the importance of model testing for defining the proper setting level of the machines. The determination of the plant NPSE of a machine is a subtle process, which should include:

- the type of cavitation developments the runner or the impeller is experiencing over the operating range of interests;
- the risk of cavitation erosion associated to this type of cavitation;
- the risk of performance alteration.

However, the assessment of those cavitation developments can take benefits in a large extent by developing monitoring instrumentation for the free stream cavitation nuclei, which can influence the cavitation development, [8]. Moreover, with respect to the cavitation erosion, relevant indirect method, such as measurement of vibratory levels, can be very useful for quantifying the risk during model tests, [5]-[7], [9] and [11].

ACKNOWLEDGMENTS

I would like to acknowledge all my colleagues of the EPFL Laboratory for Hydraulic Machines. I am very grateful to all the doctorate students I had the pleasure to supervise in the field of cavitation and hydraulic machinery.

REFERENCES

[1] IEC, "*Hydraulic Turbines, Storage Pumps and Pump-Turbines-Model Acceptance Tests*". IEC 60193 Standard, International Electrotechnical Commission; Genève, Nov. 1999.

[2] Arn C., Avellan F., Dupont P.; "Prediction of Francis Turbines Efficiency Alteration by Traveling Bubble Cavitation", *Proc. 19th IAHR Symp. Hydraulic Machinery and Systems*, Vol. 1, pp. 534 543, Singapore, 9-11 Sept. 1998.

[3] Avellan, F., Henry, P.; "Theoretical and experimental study of the inlet and outlet cavitation in a model of a Francis turbine", *Proceedings of 12th I.A.R.H. Symposium on Hydraulic Machinery in the Energy Related Industries*, paper 1-3, pp 38-55, Stirling, August 1984.

[4] Avellan, F., Gindroz, B., Henry, P., Bachmann, P., Vullioud, G., Wegner, M.; "Influence de la chute d'essai et de la nucléation sur les performances en cavitation des modèles de turbines Francis", *Proceedings of 13th I.A.H.R. Symposium on Progress in Technology*, vol. 1, pp 2.1-2.15, Montréal, September 1986.

[5] Avellan, F., Dupont, Ph.,Farhat, M.; "Cavitation Erosion Power", *Proceedings of the First ASME-*

JSDME Fluids Engineering Conference, FED-Vol. 116, pp. 135-140, Portland, Oregon, USA, 23-27 June 1991.

[6] Bourdon, P., Simoneau, R., Lavigne, P., "A vibratory approach to the detection of erosive cavitation", *Proc. of International Symposium on Cavitation Noise and Erosion in Fluid Systems, ASME Winter Annual Meeting*, San Francisco (USA), FED: Vol. 88, Dec 1989, pp 95-102.

[7] Bourdon P., Farhat M., Simoneau R., Pereira F., Dupont Ph., Avellan F., Dorey J.-M.; "Cavitation Erosion Prediction on Francis Turbines Part 1: Measurements on the Prototype", *Proceedings of the 18th IAHR Symposium on Hydraulic Machinery and Cavitation*, Valencia, Spain, Vol. 1, pp. 534-543, September 1996.

[8] Brand, C., Avellan, F.; "The IMHEF system for cavitation nuclei injection", *16th Symposium of the IAHR section on Hydraulic Machinery and Cavitation*, São Paolo (Brazil), 14-18 September 1992.

[9] Dorey J.-M., Laperrousaz E., Avellan F., Dupont Ph., Simoneau R., Bourdon P.; "Cavitation Erosion Prediction on Francis Turbines Part 3: Methodologies of Prediction", *Proceedings of the 18th IAHR Symposium on Hydraulic Machinery and Cavitation*, Valencia, Spain, Vol. 1, pp. 564-573, September 1996.

[10] Dupont P., Parkinson E., Avellan F., Walther W.; "Cavitation development in a centrifugal pump: numerical and model tests predictions", *Proc. Symp. of Cavitation Inception, ASME Winter Annual Meeting*, FED-Vol. 177, pp. 63-72, New-Orleans, USA, Nov. 28-Dec. 3, 1993.

[11] Dupont Ph., Caron J.-F., Avellan F., Bourdon P., Lavigne P., Farhat M., Simoneau R., Dorey J.-M., Archer A., Laperrousaz E., Couston M.; "Cavitation Erosion Prediction on Francis Turbines Part 2: Model Tests and Flow Analysis", *Proceedings of the 18th IAHR Symposium on Hydraulic Machinery and Cavitation*, Valencia, Spain, Vol. 1, 574-583, September 1996.

[12] Favre, J. N., Avellan, F., Ryhming, I. L., "Cavitation performance improvement by using a 2-D inverse method of hydraulic runner design", *Proceedings of International Conference on Inverse Design Concepts and Optimization in Engineering Sciences-II (ICIDES),* pp.15-1, 15-15, Pennsylvania State University (USA), October 1987.

[13] Gindroz, B., Avellan, F., Henry, P.; "Similarity rules of cavitation tests: the case of the FRANCIS turbine", *Proceedings of 14th I.A.H.R. Symposium on Hydraulic Machinery: Progress within Large and High Specific Energy,* pp. 755, 766, Trondheim (Norway), June 1988.

[14] Gindroz, B., Avellan, F., "Règles de similitude dans les essais de cavitation", *Comptes rendus des XX^{e} Journées de l'Hydraulique de la Société Hydrotechnique de France,* Papier I.18, pp. 1 - 8, Lyon (France), avril 1989.

[15] Gindroz, B., Avellan, F., Henry, P.; "Guide lines for performing cavitation tests", *Proceedings of IAHR 15th Symposium on Modern Technology in Hydraulic Energy Production,* Vol. I, paper H1, 11 pages, Belgrade, Yugoslavia, 11-14 September 1990.

[16] Gindroz, B., Henry, P., Avellan, F.; "Francis cavitation tests with nuclei injection", *16th Symposium of the IAHR section on Hydraulic Machinery and Cavitation*, São Paolo (Brazil), 14-18 September 1992.

[17] Henry, P, "Influence of the amount of bubble nuclei on cavitation tests of a Francis turbine", *Proc. of the ASME Symposium, Cavitation and Polyphase Flow Forum*, pp. 23-28, Fort Collins, 12-14 June 1978.

[18] Henry, P.; *"Turbomachines hydrauliques. Choix illustré de réalisations marquantes"*, Presses polytechniques et universitaires romandes, 412pages, Lausanne, 1992.

[19] Holl, J. W., Wislicenus, G. F.; "Scale effects on cavitation", ASME, Journal of basic Engineering, pp 385-398, 1961.

[20] Jacob, T., Prenat, J. E.; "Generation of hydro-acoustic disturbances by a Francis turbine model and dynamic behavior analysis", *Proceedings of IAHR 15th Symposium on Modern Technology in Hydraulic Energy Production*, Vol. 2, paper T4, Belgrade, Yugoslavia, 11-14 September 1990.

[21] Jacob, T., Prenat, J. E.; "Generation of hydro-acoustic disturbances by a Francis turbine model and dynamic behavior analysis", *Proceedings of IAHR 15th Symposium on Modern Technology in Hydraulic Energy Production*, Vol. 2, paper T4, Belgrade, Yugoslavia, 11-14 September 1990.

[22] Strohmer, F., Nichtawitz, A., "Influence of the dissolved air content and head on cavitation test of bulb turbine", *Proceedings of 14th I.A.H.R. Symposium on Hydraulic Machinery: Progress within Large and High Specific Energy,* pp. 779, 786, Trondheim (Norway), June 1988.